Improved Fine-Scale Laser Mapping of Component SEE Sensitivity

Andrew M. Chugg, *Member, IEEE*, Jonathan Ward, James McIntosh, Nathan Flynn, Peter H. Duncan, Thomas S. Barber and Christian Poivey, *Member, IEEE*,

Abstract— We have devised, implemented and demonstrated new scanning technology, smoother scanning algorithms and a capability to read selectable sub-sections of memory devices in order to accelerate laser SEE testing and address descrambling for interpreting MCU's and burst errors.

***Index Terms*— Semiconductor device radiation effects, Pulsed lasers, Piezoelectric transducers**

I. Introduction

EXCELLENT laser SEE mapping results have been achieved by various organisations using arrays of focused laser pulses to map the SEE sensitivity of microchips, including SEU and latchup in memories [1-2], sensitive volumes in analogue devices [3-4] and SEB sensitivity in MOSFET's [5]. However, constraints on the accuracy, reproducibility and evenness of laser pulse arrays delivered using current scanning technology and scanning patterns need to be mitigated in order further to improve the efficiency of laser SEE mapping. This paper describes some constraints and demonstrates how they may be overcome with a more flexible and precise positioning system delivering pulse arrays along curved trajectories. In an example case of laser mapping of SEE sensitivity in memories, the acceleration and smoothing of the scanning technology also necessitates the reading of targeted patches within memory devices in order to perform read-cycles frequently enough to exceed the laser pulsing rate. This is required in order to associate a specific memory error with a particular laser pulse. In another example, the continuous laser Single Event Transient (SET) scanning of amplifiers puts intensive demands on digital oscilloscope technology, since it requires that large numbers of SET events be captured at a high rate.

The traditional approach has been raster scanning of the device under test using stepper-motor driven positioning systems. Much good research has been achieved with such systems, but there is a recognition that improvements are possible and should be pursued. For example, French experimenters are currently applying new types of laser scanning of microchips: e.g. in Fig. 2 of [8] an alternative optical setup employs an X-Y scanner that allows fast scanning of small areas using steering mirrors (without moving the device). This paper focuses upon the application of curvilinear scanning trajectories and continuous (piezoelectric) positioning systems and the improvements of laser SEE sensitivity mapping that they facilitate.

Manuscript received 2nd September, 2011.

This work was supported by the European Space Agency under Phase 5 of ESTEC Contract No. 16916/02/NL/PA

A. M. Chugg, J. Ward, J. McIntosh, N. Flynn, P. Duncan & T. Barber are with the Radiation Effects Group, MBDA UK Ltd., Z12, PO Box 5, Filton, Bristol BS34 7QW, UK, email: Andrew.chugg@mbda-systems.com

Christian Poivey is with the European Space Agency, ESTEC, Keplerlaan 1, PO Box 299, 2200 AG Noordwijk ZH, Netherlands.

II. New Approaches and Techniques

A. Piezo-Electric Positioning

Stepper motor positioning systems are constrained by a finite step size and cumulative positioning errors. Each move has distinct phases of acceleration followed by constant velocity followed by deceleration, which makes it difficult to implement curvilinear trajectories smoothly. In general, a raster scanning pattern is used with sharp decelerations and accelerations at the ends of each row that tend to induce vibrations in the mount. Since lasers need to operate at a fixed pulse repetition rate for optimal pulse stability, lacking any mitigation, stepper motor arrays would deliver denser patterns of laser pulses at the ends of each row (Fig. 1) with reproducibility that is limited by the magnitude of the induced vibration and cumulative errors from missed steps and mechanical slack at the reversals.

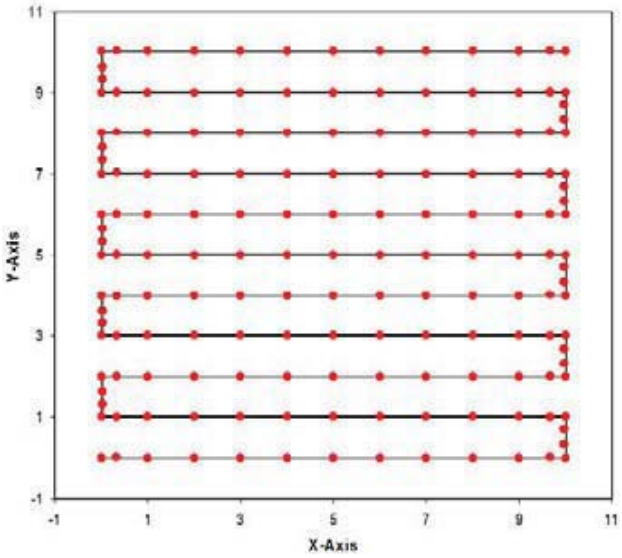

Fig. 1. Clustering of laser pulses at the ends of rows in a raster scanning pattern (conceptual).

978-1-4577-0587-8/11/$26.00 ©2011 IEEE

It is, of course, possible to mitigate these issues in many ways and this is what happens in practice. For example, the lasing can be interrupted or masked at the end of every row. However, it would potentially be more efficacious to adopt an area-scanning trajectory that minimizes accelerations, whilst maintaining an even density of laser pulses. A particular spiral trajectory, when scanned at constant speed, can be shown to satisfy these requirements, but it is extremely difficult to implement spiral scanning on a scale of micrometers using stepper motor technology.

In the field of scanning electron microscopy the exceptional accuracy requirements for positioning and translation have led to the development of piezo-electric actuated positioning systems. Therefore, in our research we have pursued the introduction of this technology to augment our existing nanostep motors in our SEREEL2 laser SEE simulation facility.

The new system is outlined in Fig. 2. It may be controlled by LabVIEW software. The x and y displacements are smooth and continuous and proportional to the voltages applied to each axis. Hence curvilinear trajectories may be implemented by downloading any desired waveform into the Arbitrary Waveform Generator for analogue conversion and thence into the x and y-axis servo controllers respectively for application to the piezo-actuators themselves. The system also includes Strain Gauge Sensors (SGS's), which monitor the actual physical displacements of the piezo-actuators and provide a feedback loop. The SGS feedback signal can be used to monitor and continuously correct the performance of the system, thus largely removing positional uncertainties.

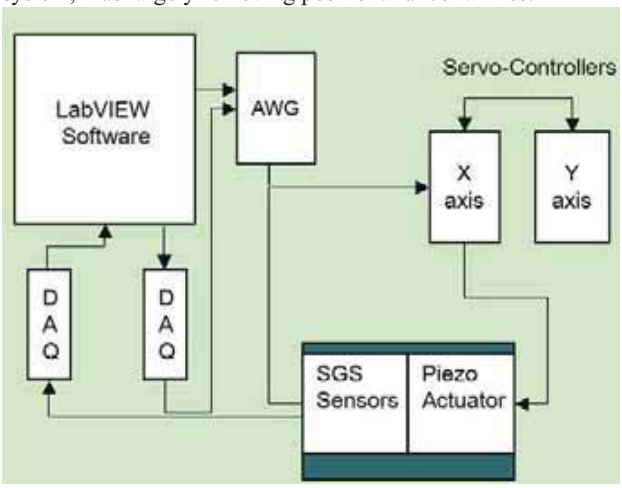

Fig. 2. Piezo-actuator control loop.

B. Spiral Scanning Trajectories

Given a fixed laser repetition rate, how can an area of a microchip be scanned so as to produce an evenly spaced array of laser pulses? This objective requires that the scanning pattern trajectory be performed at constant speed, so that the spacing of laser pulses along the trajectory is equal. This means that the trajectory must be curvilinear, because any sharp changes in the direction of the trajectory will either require a speed reduction or will give a sharp spike of acceleration that will induce vibrations in the mount. In order evenly to fill an area with a laser pulse array, the trajectory must also veer back past its previous path at a spacing roughly equal to the spacing of pulses along the path. A practicable solution to these two criteria is a spiral trajectory defined by the following x and y equations of the time parameter:

$$x = A\sqrt{t}\cos(\omega\sqrt{t}) \quad (1)$$

$$y = A\sqrt{t}\sin(\omega\sqrt{t}) \quad (2)$$

These give a constant trajectory speed around the spiral, where A and ω are fitting parameters to scale the spiral array appropriately in a given application. It can be shown that ω is defined by the laser pulse repetition period Δt_p as follows:

$$\Delta t_p = \frac{4\pi}{\omega^2} \quad (3)$$

Hence ω is defined by the laser pulsing rate. The A parameter can be defined in terms of the time to deliver the array t_{max} and the maximum radius of the array r_{max} using the relations:

$$t_{max} = \left(r_{max} / A \right)^2 \quad (4)$$

For the example array shown in Fig. 3, A=1 and ω=1 with t_{max}=3000s and Δt_p=10s.

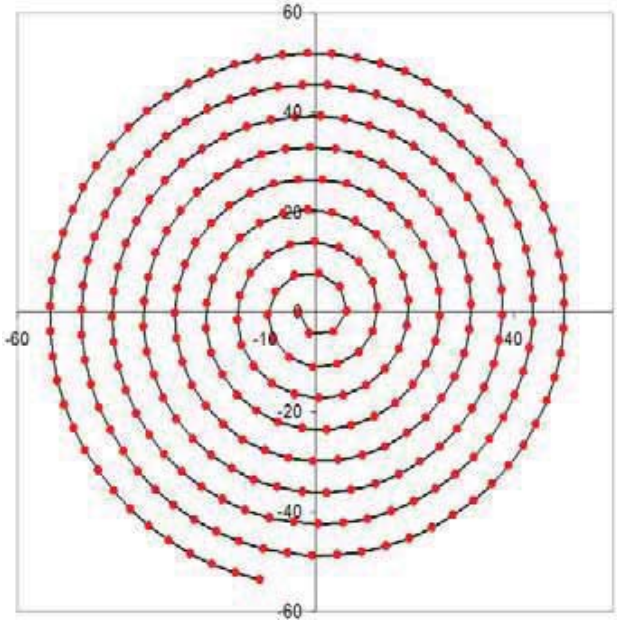

Fig. 3. A spiral laser pulse array (conceptual).

C. Compacted Memory Patch Read/Write System

It is necessary to read the monitored set of memory bits at least once within the period between successive laser pulses, so that an observed error can be attributed to a particular laser pulse. Since it is proposed to pulse the laser at up to 100Hz during automated laser SEE sensitivity mapping, the entire memory cannot be read fast enough to keep up with the pulses

in the case of megabit devices. The current read-cycles for megabit memories with MBDA's standard STREAM test kit (a proprietary FPGA-based system for reading memories and correcting errors during testing) are of the order of seconds. This needs to be reduced to of the order of milliseconds, implying a thousand-fold reduction in the number of bits read during sensitivity mapping.

This has been achieved by fixing a subset of the address lines at pre-set values, so as to treat the device as a smaller sized memory corresponding to the number of the remaining set of address lines. In order to choose the correct set of address lines to target a specific patch, it is necessary to have a large scale descrambling of address lines to corresponding physical locations on the chip. Of course, this is something that is easily accomplished with a laser SEE system. In this way it is possible to read solely bits within an identified rectangular patch. As an example, Fig. 4, which shows how a subset of the address lines (A0,A1,A2,A16,A17,A18) can be fixed in different patterns to address bits in two different patches of the Alliance AS7C34096A SRAM, which was used for the initial laser SEE experiments conducted for this research.

Another constraint was that the STREAM system had a mass of 600g, which is too heavy to be mounted on the delicate piezo-electric positioning system. Consequently, a compact STREAMlite card was developed with a mass of less than 100g to support future laser investigations in memories.

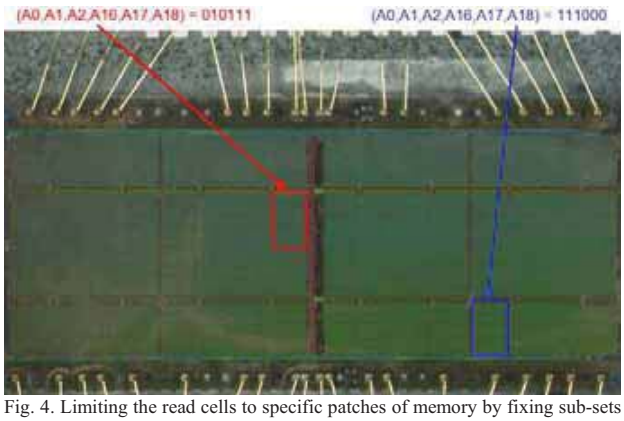

Fig. 4. Limiting the read cells to specific patches of memory by fixing sub-sets of the address lines.

III. SRAM SEE Sensitivity Mapping

A backside polished sample of the Alliance AS7C34096A SRAM has been used to validate the new techniques in the context of an actual memory microchip. This is one of the devices currently being flown in ESA's Proba 2 spacecraft in the Technology Demonstrator Module [6-7]. Arrays of 300 laser pulses were delivered at 100Hz pulse repetition rate (i.e. the run duration was 3s). The targeted memory patches were read at approximately 200Hz so as to associate each observed error with a specific laser pulse. The diameter of the arrays was ~25μm and the laser pulses had a separation of ~1μm.

The observed Single Event Upset (SEU) locations for a delivered spiral array of laser pulses are plotted on the scanning path in Fig. 5, where the errors have been colour-coded depending on whether a selected address bit of the errors was 1 (blue) or 0 (green). Note that the sample was oriented slightly obliquely during the trial. There were virtually no errors down the left-hand side of the array, since this was deliberately made to overlap a region of address lines and control logic that was relatively insensitive to laser pulses. The most impressive result of the experiment was the relatively clear stripes of 1's and 0's in the individual error address bits. This immediately revealed the fine-scale organization of the memory, which turns out to be controlled by address bits A7 to A12 for this device. The memory cell dimensions for this device are identified as in the micrograph as 1.7μm x 2.52μm, which is perfectly in line with the laser trial data (the inferred vertical and horizontal memory cell divisions have been sketched onto the A11 and A7 address bit error distributions in Fig. 5 to clarify this point.)

The descrambling information is valuable in SEE testing, because it can be used to plot the physical location of MCU's and burst errors. Both of these phenomena are rapidly growing in importance and there is special research interest in investigating the physical distributions of burst errors at this time in order to determine which design features of SDRAM's and SRAM's might be responsible.

The spiral array has been delivered at a range of laser pulse energies, so as to derive an SEU sensitivity map for the exposed region. The results are shown in Fig. 6, where the size of the spots indicates the sensitivity at each location. (There are more points on this plot than were delivered in a single run, because some of the arrays were slightly offset from the others due to systematic errors.) The insensitive region to the left of the memory cell array is evident. There is also good evidence for a wide range of sensitivity within memory cells, since there is a wide range of sensitivity thresholds across the memory cell region. However, due to the small size of the cells, there were only a few laser pulse locations within each cell, so the details of the variation within cells cannot be resolved. Previous work [1] has shown that strong sensitivity variations can exist between rows of cells, but the Alliance sample exhibited similar SEU sensitivity ranges in all the exposed cells.

IV. SET Mapping in an Amplifier

Recent Single Event Transient (SET) sensitivity mapping performed by MBDA provides a contrasting and complementary example of the spiral trajectory mapping in practice. This was conducted upon the familiar National Semiconductor LM124J amplifier device that has large feature size metallization tracks, which provide an excellent mask over SEE sensitive features in the laser pulse array, so that the correctness of the registration of the laser pulse array with device features is readily verified.

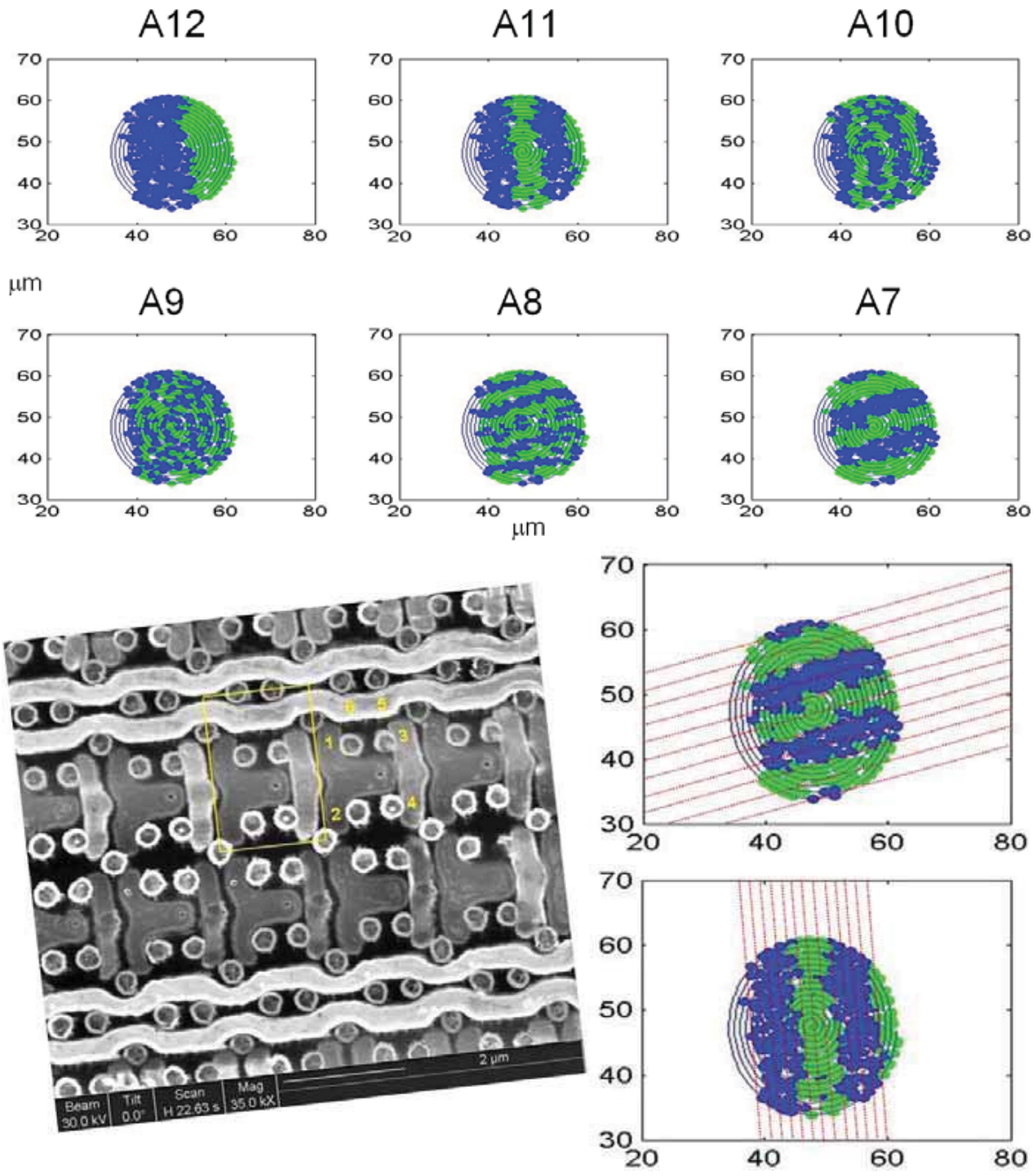

Fig. 5. Laser-induced SEU's in the Alliance AS7C34096A colour-coded according to the values of address bits revealing the fine-scale memory organization.

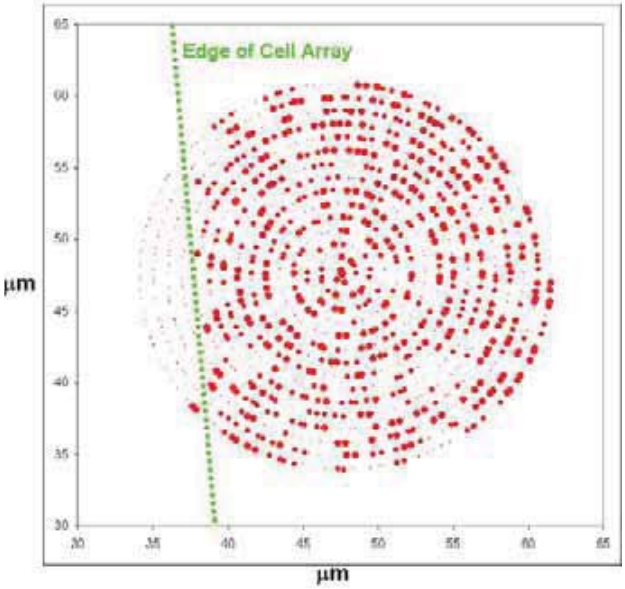

Fig. 6. Observed SEU sensitivity variations across the laser pulsed region.

In the experimental configuration a Tektronix TDS5104 oscilloscope was triggered off the same pulse stream that was used to trigger the laser pulses (1064nm wavelength and 400ps pulse duration). The rate at which this item of equipment was able to capture SET events with time resolution of 80ns and the total amount of active storage memory available were the main limitations on the laser pulse frequency and the total number of pulses delivered in an array. A pulse repetition frequency of 10Hz was consequently adopted for this research with 122 laser pulses delivered in 12.2s. The arrays had a radius of ~50µm, which corresponds to the amplitude limit of the current piezo-electric X-Y positioners. The overall experimental coordination was performed by purpose-written LabVIEW instrument control software.

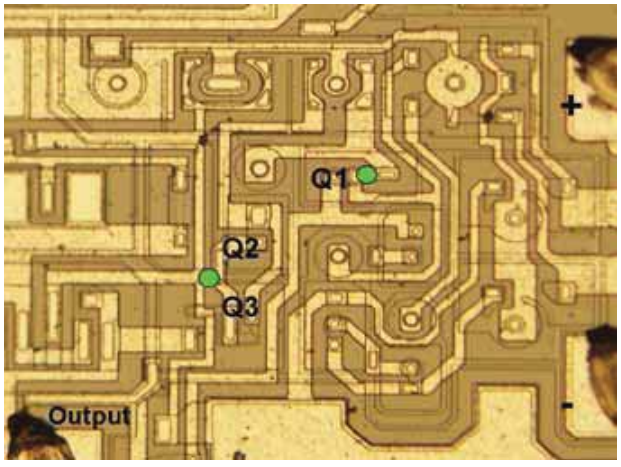

Fig. 7. One of the four independent high gain op-amps on the National Semiconductor LM124J: green spots show lasing centers for labeled transistors Q1-Q3.

Copious amounts of data are gathered in performing this research, but only a few characteristic example cases may be presented here. Fig. 7 shows the lasing locations corresponding to the data presented in this paper. Fig 8 is a representative range of examples from the group of SET's gathered when the laser pulse array (pulse energy = 5pJ) was delivered across the region of the transistor labeled Q1 in Fig. 7 on the amplifier. The array is plotted in Fig. 9 with the laser pulse locations as read from the strain gauge sensors. A microscope view of the corresponding surface area of the amplifier is shown in the background. The small white spots in Fig. 9 mark pulse locations where any SET was small enough to be lost in the noise. However, wherever a SET of significant amplitude relative to the nominal output level was observed, a red spot is shown with a radius proportional to the peak deviation of the output voltage from nominal.

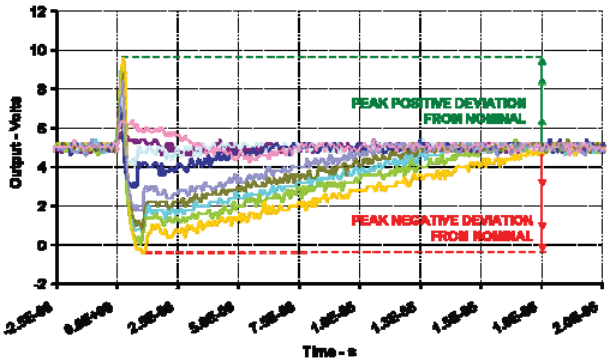

Fig. 8. Examples from a group of SET's gathered in laser mapping the vicinity on the transistor labeled Q1 on an LM124 at low laser pulse energy (5 pJ).

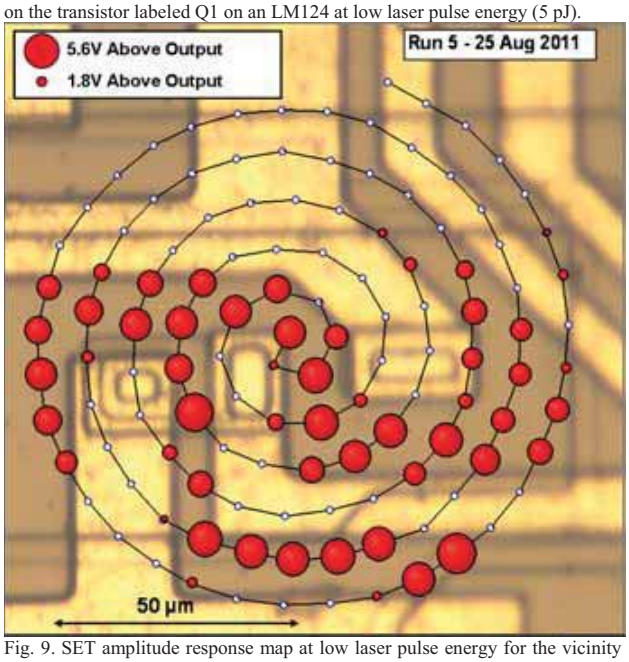

Fig. 9. SET amplitude response map at low laser pulse energy for the vicinity on the transistor labeled Q1 on an LM124 (red spots plotted at size proportional to amplitude – white spots are zero SET amplitude locations.)

It is notable that there is a high degree of correspondence between the large amplitude SET's and the regions of exposed silicon, but some SET's were also seen near the edges of the

metallization. This is attributable to a combination of factors: the finite width of the laser spot, a residual positional error of the order of 1□m (as also seen in the SRAM mapping) and very high SET sensitivity at some points near the edge of the metallization, where it masks a particularly sensitive area.

There are also some regions of the silicon that are insensitive to SET's at this pulse energy, especially in the upper right part of the laser pulse array. However, these regions also become sensitive for the group of SET's gathered from the same region at higher laser pulse energy (60pJ). A sub-set of these are shown in Fig. 10, where it can be seen that some of the SET's are starting to hit the positive power rail near +15V. The positions and magnitudes of these SET's are plotted in Fig. 11. Virtually all the exposed silicon now exhibits SET sensitivity and the incursions of sensitivity over the edges of the metallization are seen to be exacerbated.

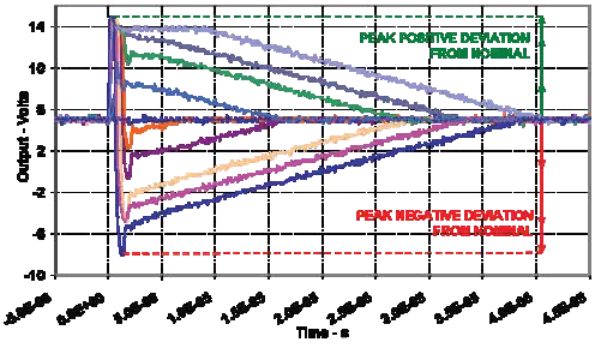

Fig. 10. Examples from a group of SET's gathered in laser mapping the vicinity of transistor Q1 on an LM124 at high laser pulse energy (60pJ).

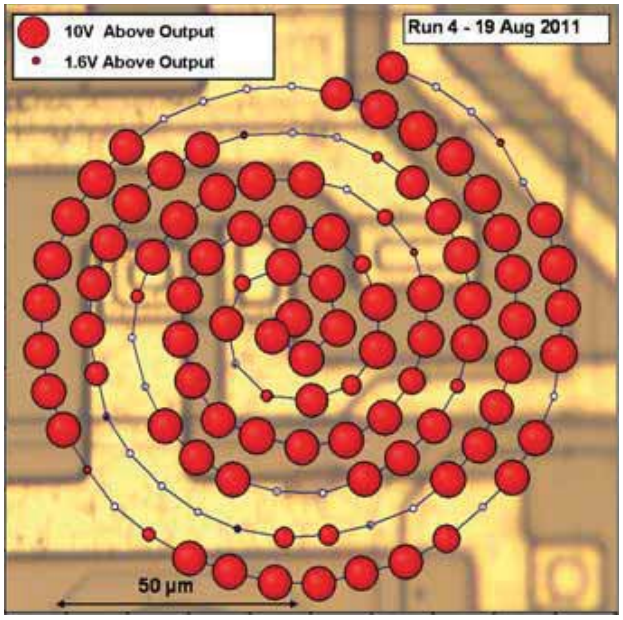

Fig.11. SET amplitude response map at high laser pulse energy for the vicinity of transistor Q1 on an LM124 (red spots plotted at size proportional to amplitude – white spots are zero SET amplitude locations.)

A range of different forms of SET are seen in both Fig. 8 and Fig. 10: for example, some SET's show only positive deviations from nominal, whilst others show positive deviations followed by negative ones. This can be shown to correspond to different regions of sensitivity on the face of the microchip. This can be illustrated with a third example case for a different area of the amplifier.

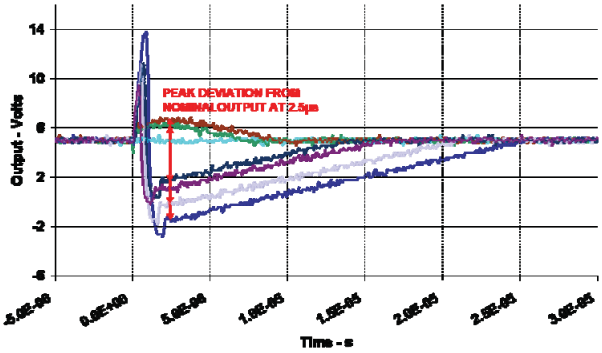

Fig. 12. Examples from a group of SET's gathered in laser mapping the vicinity of transistors Q2 and Q3 on an LM124 at laser pulse energy 50 pJ.

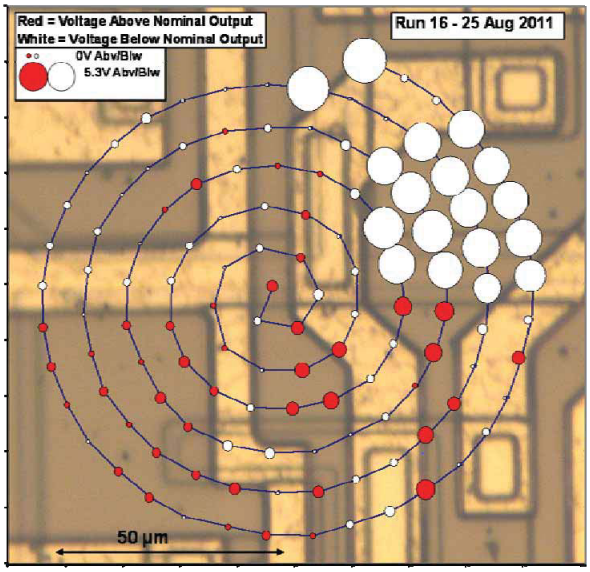

Fig. 13. SET amplitude response map at 2.5µs post-pulse for the vicinity of transistors Q2 and Q3 in Fig. 7 on an LM124 (red spots for positive deviations and white for negative deviations plotted at size proportional to amplitude.)

Another group of SET's, plotted in Fig. 12, was gathered across the boundary between Q2 and Q3 on Fig. 7. Some of these SET's exhibited a secondary positive hump at ~2.5µs after the laser pulse. This SET array is plotted in Fig. 13, where the radius of the spots is proportional to the magnitude of the SET deviation from nominal at 2.5µs with the innovation that a positive deviation is colored red and a negative deviation is shown in white. This makes it immediately clear that the large negative deviations all derive from a distinct region in the upper right of the array (corresponding to transistor Q2), whereas the transients with the secondary positive humps are associated particularly with the adjoining transistor Q3.

V. Discussion

The illustrative results that have been presented are evidence that this is an efficacious technique for laser SEE sensitivity mapping, but the key point is that the barriers to further improvements in efficiency and accuracy are lower than for raster scanning using stepper motors (although those techniques can be and have been used to obtain similar results).

The question of accuracy is different for this technique than for conventional stepper motor positioning, because the actual location of the array is read from the strain gauge sensors at every point. Positional errors due to stepper motor backlash, missed steps and similar (often cumulative) errors are therefore not an issue, but there is still some inaccuracy attributable to strain gauge noise and the accuracy with which the laser pulses can be located on the trajectory read from the strain gauges.

A related issue is the reproducibility of the array for runs at a range of different pulse energies. Our system currently gives a reproducibility error of around 1μm, so long as the microchip under test is not repositioned between runs. This is already smaller than the laser spot diameter and can potentially be improved further. If repositioning (or any mechanical jogging of the setup) intervenes, then the reproducibility will be less accurate.

Of course microchips are usually rectangular and the spiral array is virtually circular. However, we retain a stepper motor system for large scale positioning, since the piezoelectric system is currently limited to 100μm of travel in X and Y. It is also possible to perform a raster scan with piezoelectric system. Often a circular mapping region will fit sub-features of interest just as well as a raster scan. It may be an advantage that it is impossible for the spiral laser spot array to become aligned with the (usually) rectilinear features of a microchip design, because such alignments may sometimes allow significant sensitive features to be missed between the scan lines.

VI. Conclusion

This paper has described the design, implementation and validation of a scanning system designed to improve the automated SEE sensitivity mapping of microchips with focused laser pulses. This has been demonstrated by fine-scale laser SEE mapping an SRAM and SET mapping of sub-regions of an LM124 amplifier. The combination of accuracy and speed facilitates high volume laser screening of small feature size parts and the technology is scaleable to yet higher laser pulse frequencies and larger laser pulse arrays. The descrambling data obtained for the SRAM is also valuable for interpreting the MCU and burst errors increasingly seen in SEE testing.

References

[1] A.M. Chugg, A.J. Burnell, M.J. Moutrie, R. Jones and R. Harboe-Sørensen, “Laser SEE Sensitivity Mapping of SRAM Cells”, IEEE Trans. on Nucl. Sci., Vol. 54, No. 6, pp2106-2112, December 2007.

[2] A.J. Burnell, A.M. Chugg and R. Harboe-Sørensen, “Laser SEL Sensitivity Mapping of SRAM Cells”, IEEE Trans. on Nucl. Sci., Vol. 57, No. 4, pp. 1973-1977, Aug. 2010.

[3] D. McMorrow, W.T. Lotshaw, J.S. Melinger, S. Buchner, Y. Boulghassoul, L. Massengill, R.L. Pease, “Three-dimensional mapping of single-event effects using two photon absorption”, IEEE Trans. on Nucl. Sci., Vol.: 50, Issue: 6, Part: 1, pp2199–2207, December 2003.

[4] Cecile Weulersse, Francoise Bezerra, Florent Miller, Thierry Carrière, Nadine Buard, and William Falo, “Probing SET Sensitive Volumes in Linear Devices Using Focused Laser Beam at Different Wavelengths”, IEEE Trans. on Nucl. Sci., Vol. 55, No. 4, pp.2007-2012, August 2008.

[5] F. Miller, A. Luu, F. Prud’homme, P. Poirot, R. Gaillard, N. Buard, and T. Carrière, “Characterization of Single-Event Burnout in Power MOSFET Using Backside Laser Testing”, IEEE Trans. On Nucl. Sci., Vol. 53, No. 6, pp. 3145-3152, Dec. 2006.

[6] R. Harboe-Sørensen, C. Poivey, F.-X. Guerre, A. Roseng, F. Lochon, G. Berger, W. Hajdas, A. Virtanen, H. Kettunen, S.Duzellier, “From the Reference SEU Monitor to the Technology Demonstration Module On-Board PROBA”; IEEE Trans. on Nucl. Sci Volume 55, Issue6, Part 1, pp3082 – 3087, Dec. 2008.

[7] R. Harboe-Sørensen, C. Poivey, N. Fleurinck, K. Puimege, A. Zadeh, F.-X. Guerre, F. Lochon, M. Kaddour, L. Li, D. Walter, A. Keating, A. Jaksic, & M. Poizat, “The Technology Demonstration Module On-Board PROBA-II”, currently (6/4/11) accepted for a future issue of TNS and online at IEEE Xplore.

[8] E. Faraud, V. Pouget, K. Shao, C. Larue, F. Darracq, D. Lewis, A. Samaras, F. Bezerra, E. Lorfevre & R. Ecoffet, “Investigation on the SEL Sensitive Depth of an SRAM using Linear and Two-Photon Absorption Laser Testing”, presented at NSREC 2011.